Effect of a Zirconium Tungstate Filler on the Cure Behavior of a Cyanate Ester Resin

K. Haman, P. Badrinarayanan, and M. R. Kessler*

Department of Materials Science and Engineering, Iowa State University, 2220 Hoover Hall, Ames, Iowa 50011

ABSTRACT In this work, the effect of a negative thermal expansion zirconium tungstate (ZrW_2O_8) filler on the cure behavior of a unique low-viscosity bisphenol E cyanate ester (BECy) is characterized by differential scanning calorimetry. The cure rate of BECy is found to increase upon the incorporation of ZrW_2O_8 particles, and the catalytic effect increases with increasing filler loading. The catalytic effect is primarily attributed to the presence and nature of hydroxyl groups on the ZrW_2O_8 particle surface. In comparison with BECy/ZrW_2O_8 composites of the same loading, silane-coated ZrW_2O_8 particles resulted in a higher value of the glass transition temperature (T_g) and a delay in the onset of the cure. The ability of a phenomenological reaction model to describe the cure behavior of the composites is also examined.

KEYWORDS: zirconium tungstate • thermosets • DSC • cure kinetics

1. INTRODUCTION

Bisphenol E cyanate ester (BECy) is a unique resin that is ideally suited for use in polymer matrix composites (1, 2). Unlike other cyanate ester and epoxy monomers, BECy exhibits low viscosity (0.09 Pa · s) at ambient temperatures (3), which is conducive for the incorporation of filler particles. Furthermore, BECy cures by cyclotrimerization (2), as demonstrated in Figure 1, and forms a cross-linked thermoset with a high glass transition temperature (T_g). Hence, recent work has focused on the development of high-performance composite materials through the incorporation of various fillers in BECy such as fumed silica (4), alumina nanoparticles (5), and zirconium tungstate (6).

Filler materials are employed to tailor the thermal, mechanical, rheological, and dielectric properties of polymer resins (7). Achievement of the desired property enhancements is often determined by the degree of interaction and the interface between the filler particles and the polymer matrix (7). Although several researchers have investigated the cure kinetics of cyanate ester resins, the number of studies on the cure behavior of filler-reinforced cyanate ester composites is limited. Ganguli and co-workers (8) reported that silicate clay nanoparticles catalyzed the cure of a cyanate ester resin. Kissounko and co-workers (9) reported that the initial cure rate of a cyanate ester doubled upon the addition of clay nanoparticles. Goertzen and co-workers (4) reported that silica nanoparticles catalyzed the cure reaction of the BECy resin. In recent work, Sheng (5) found that the incorporation of alumina nanoparticles resulted in a catalytic effect on the cure kinetics of BECy; the increase in the cure rate was attributed to the presence of hydroxyl groups on particle surfaces and the Lewis acidity of the γ-phase alumina. In this work, we investigate whether the cure kinetics of BECy are influenced by zirconium tungstate filler reinforcements, which also possess surface hydroxyl groups (10).

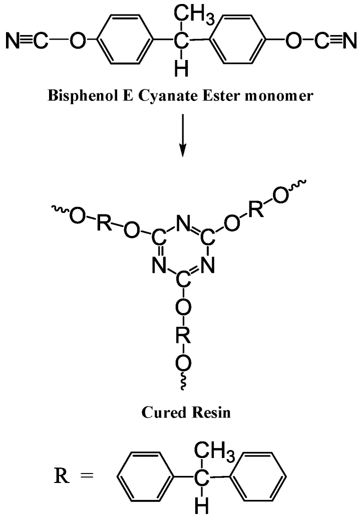

FIGURE 1. Cyclotrimerization reaction of BECy.

Zirconium tungstate (ZrW_2O_8) is a ceramic material that exhibits strongly negative isotropic thermal expansion over a wide temperature range, reported between 20 and 950 K (11−14). The negative coefficient of thermal expansion (CTE) behavior in ZrW_2O_8 arises as a consequence of transverse vibrations exhibited by oxygen atoms that connect zirconium oxide octahedra with tungsten oxide tetrahedra; these vibrations cause the polyhedra to rotate, resulting in the structure receding inward and leading to an overall reduction in size (11−14). The values of the CTE for ZrW_2O_8 can range from -8.7×10^{-6} to -1×10^{-6} K^{-1}, depending on the temperature and pressure (11). Consequently, a few studies in the literature (15−19) have reported that the CTE of polymer matrix composites can be tailored through the incorporation of various amounts of ZrW_2O_8. In recent work (6), the incorporation of micrometer-sized ZrW_2O_8 has been

---

* Corresponding author. E-mail: mkessler@iastate.edu. Phone: 515-294-3101. Fax: 515-294-5444.

Received for review January 24, 2009 and accepted April 25, 2009

DOI: 10.1021/am900051g

found to result in dramatic reductions in the CTE of BECy. Furthermore, the storage modulus was also found to increase with ZrW_2O_8 filler loading, although the glass transition temperature (T_g) of the composite was found to decrease when determined by thermomechanical analysis. Various applications have been projected for the low-CTE ZrW_2O_8/polymer matrix composites such as adhesives, optical mirrors, and circuit boards (15, 17, 19). However, to the best of our knowledge, the impact of the ZrW_2O_8 filler on the thermoset resin cure behavior has never been examined.

The thermomechanical properties of a composite are significantly influenced by the resin cure conditions; hence, a detailed understanding of the effect of ZrW_2O_8 filler loading on the cure of the BECy resin is crucial to optimizing the properties of a high-performance thermoset and the cure schedules. The objective of this work is to examine, for the first time, the effect of ZrW_2O_8 filler loading on the cure kinetics of a BECy resin by differential scanning calorimetry (DSC) measurements. Furthermore, because one study (18) in the literature has reported that significant improvements in the thermomechanical properties of thermoset resins are possible through the surface treatment of ZrW_2O_8, we also examine the impact of a silane surface treatment of ZrW_2O_8 on the T_g and cure behavior of BECy composites.

The reaction conversion or degree of cure of a resin can be monitored by performing a dynamic scan at a constant heating rate. The cure reaction of a thermoset manifests as an exotherm in the heat-flow signal measured by DSC, and the degree of conversion (α) from the BECy monomer (where $\alpha = 0$) to a fully cross-linked polymer network (where $\alpha = 1$) can be determined as shown in eq 1

$$\alpha(t) = \frac{H(t)}{H_R} \tag{1}$$

where H_R is the total enthalpy of the reaction obtained by integration of the total area under the heat-flow curve and $H(t)$ is the enthalpy of the reaction at time t (20). The nature of cure reactions can be further examined through model fits of DSC data with phenomenological reaction models. In this work, the cure behavior of BECy/ZrW_2O_8 composites is examined by fitting the data from DSC measurements with an autocatalytic reaction model because the model has been found to provide an excellent description of both isothermal and dynamic DSC cure measurements of BECy in previous work (2). The ability of autocatalytic reaction models to describe cyanate ester cure kinetics has also been demonstrated by Chen and co-workers (21) and by several early reports in the literature, which are described elsewhere (22).

2. METHODOLOGY

2.1. Materials. The bisphenol E cyanate ester (BECy) used in this work was purchased from Bryte Technologies (Morgan Hill, CA) as a EX-1510 resin. Zirconium tungstate was obtained from ATI Wah Chang (Albany, OR) in the form of a powder with a reported median particle diameter of 22 μm (23) and was stored in a tightly sealed container prior to use. The density of ZrW_2O_8 was taken as 5.07 g/cm^3 (11).

2.2. Sample Preparation. Zirconium tungstate particles (10 and 20 vol %) were added to a vial containing 1.5 g of the BECy resin and dispersed by ultrasonication using a sonic probe. The filler loading is possible with relative ease because of the low ambient temperature viscosity of the EX-1510 BECy resin. The vials were also sonicated prior to each DSC measurement in order to minimize possible errors in composition due to settling of the filler particles.

2.3. DSC Measurements. Cure characterization of the BECy and BECy/ZrW_2O_8 composites was performed in a model Q20 DSC from TA Instruments (New Castle, DE). T-Zero hermetic pans (TA Instruments) were loaded with ca. 8 mg samples and cured at 5, 7, 10, and 15 K/min heating rates from room temperature to 350 or 360 °C.

Measurements of the glass transition temperature were performed in a model Q2000 DSC from TA Instruments for samples cured at 15 K/min. The sample was heated above T_g to erase the previous thermal history and was subsequently cooled at 10 K/min to 25 °C, and a second heating scan at 10 K/min was performed to 350 °C. The glass transition temperature of each sample was determined from the second heating scan as the onset point of the step change in the heat flow.

2.4. Thermogravimetric Analysis (TGA) Measurements. The filler content in each sample was examined in a Q50 thermogravimetric analyzer from TA Instruments. The measurements were performed by heating a small quantity of the sample at 20 K/min under air purge.

2.5. Silane Treatment of ZrW_2O_8. Zirconium tungstate particles were dispersed with 125 mL of distilled and dry tetrahydrofuran (THF) in a 250 mL flask by sonication in an ultrasonic bath (Branson model 1510). Next, 2.5 mL of a (glycidyloxypropyl)trimethoxysilane (GPS) solution was injected into the flask, and the mixture was refluxed for 2 days at 95 °C. The solution was centrifuged to separate the functionalized particles from the mixture. The functionalized ZrW_2O_8 (F-ZrW_2O_8) particles were washed with THF to remove excess GPS and separated from the solution by centrifugation. The particles were allowed to dry at room temperature for 2 days and subsequently dried under vacuum to remove residual solvents.

2.6. Fourier Transform Infrared (FT-IR) Measurements. The presence of hydroxyl groups in ZrW_2O_8 particles was verified through FT-IR spectroscopy measurements. The samples were prepared in the form of pellets along with potassium bromide (KBr) in a pellet press. The measurements were performed on a Vertex 70 FT-IR spectrometer from Bruker Inc. (Madison, WI).

2.7. X-ray Diffraction (XRD) Measurements. XRD measurements were performed on a Scintag XDS-2000 powder diffractometer with a Cu radiation source and an air-cooled Peltier silicon detector. A step size of 0.02° was employed.

3. RESULTS AND DISCUSSION

Zirconium tungstate can exist in three different phases and exhibits some unique behavior on heating at ambient pressures. The heat-flow curve obtained from DSC measurements of as-received ZrW_2O_8 is shown in Figure 2. An endothermic transition can be observed in the heat flow with a peak at 140 °C; this corresponds to a change in the crystal structure of ZrW_2O_8 from an orthorhombic to a cubic lattice and is known as the γ–α-phase transition, as confirmed by the calorimetric measurements of Holzer and Dunand (24). Upon heating above 150 °C, another transition from the α phase to the β phase can be observed because of a change in the crystal structure from an ordered to a disordered cubic lattice. The order–disorder transition is reversible upon cooling and occurs because of a transfer of mobile oxygen

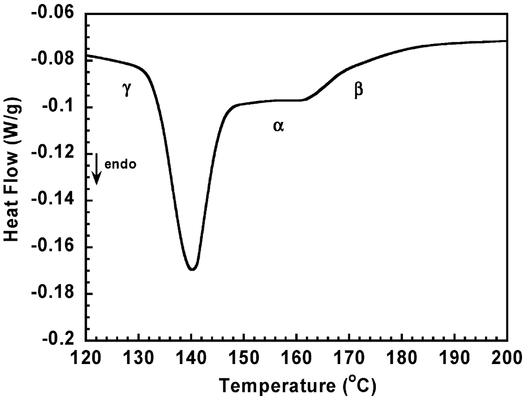

FIGURE 2. DSC thermogram showing phase transitions of ZrW_2O_8 from γ to α at 140 °C and from α to β at 160 °C.

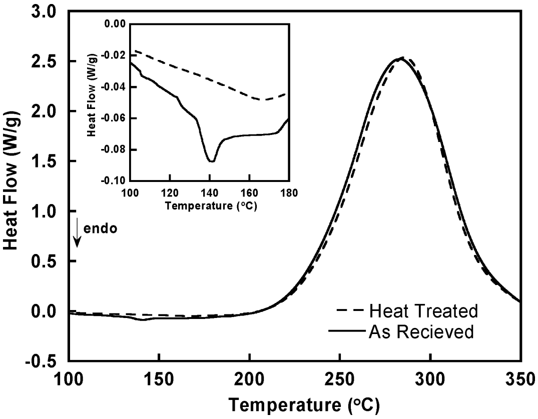

FIGURE 3. Comparison showing the effect of heat treatment on the cure kinetics of BECy/ZrW_2O_8 composites.

atoms within the structures. However, the α or β phase can be transformed to the γ phase only through application of pressures up to 200 MPa (11, 25–27). The as-received ZrW_2O_8 and heat-treated ZrW_2O_8, which was heated above the temperature range of the γ–α phase-transition, were compared by XRD measurements. Although the two powders were expected to be in different phases, i.e., γ and α, respectively, no significant difference was observed in the XRD spectra, apart from slight differences in intensity. A similar result was reported by Perrottoni and and Da Jornada (28), who suggested that, even though a pressure of 200 MPa is sufficient to induce the formation of the γ phase, marked differences in XRD or Raman spectra between the cubic α phase and the orthorhombic γ phase are observed only if the γ phase had been induced by the application of pressures on the order of 1 GPa.

In order to examine whether the phase transitions of ZrW_2O_8 have an impact on the cure of BECy, the ZrW_2O_8 powder was heated above the temperature range of the γ–α-phase transition in a convection oven so that the powder is never in the γ phase during the cure. The heat-flow curves obtained for BECy/ZrW_2O_8 composites with 10 vol % of heat-treated and as-received fillers are compared in Figure 3. The heat-flow curve of the resin with as-received ZrW_2O_8 exhibits an endotherm with a peak temperature at 140 °C due to the γ–α-phase transition, whereas the heat flow of the resin with heat-treated ZrW_2O_8 does not exhibit the γ–α-phase transition, as shown in the inset of Figure 3. Apart from this difference, no other variations in the onset or peak temperature of the cure exotherms can be observed between the two methods, suggesting that heat treatment of ZrW_2O_8 does not significantly influence the cure kinetics. This also indicates that the as-received ZrW_2O_8 particles do not contain a significant amount of adsorbed water, which would have led to some differences in the cure kinetics between the BECy resin with heat-treated ZrW_2O_8 and as-received particles. Hence, the BECY/ZrW_2O_8 composites were prepared without any additional thermal treatments for ZrW_2O_8.

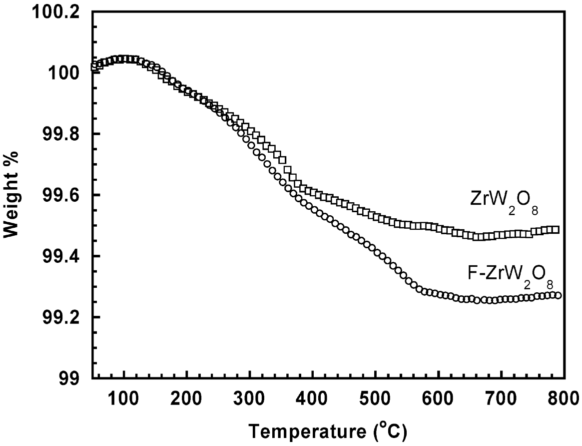

FIGURE 4. Comparison of weight loss curves between as-received ZrW_2O_8 (□) and F-ZrW_2O_8 (○).

The compositions of the composite samples were verified by TGA measurements. Upon heating to 800 °C, BECy degrades completely and ZrW_2O_8 decomposes to ZrO_2 and WO_3. The average difference in volume percent between the expected loading and the value determined from TGA is found to be less than 1 % if the weight loss of ZrW_2O_8 is also accounted for. The weight loss curves of ZrW_2O_8 and F-ZrW_2O_8 particles are shown in Figure 4. In general, for ceramic oxides such as ZrW_2O_8, the weight loss up to 200 °C may be attributed to physically adsorbed water, while any loss that occurs between 200 and 600 °C may be attributed to the loss of surface hydroxyl groups (29). On the basis of the weight loss between 200 and 600 °C, the hydroxyl group content in the ZrW_2O_8 particles may be estimated as 0.47 wt %. It is noted that the weight loss for F-ZrW_2O_8 particles up to 200 °C is found to be similar to that of ZrW_2O_8 particles, indicating no significant difference in the content of physically adsorbed water. However, the weight percent of F-ZrW_2O_8 particles is found to be lower between 200 and 600 °C when compared to that of the as-received particles because of decomposition of the organic constituents of GPS. An estimate of the OH content for the F-ZrW_2O_8 particles is difficult to obtain by TGA measurements because of the overlap of the weight loss regimes of the loss hydroxyl groups and silanes.

DSC measurements of the composite T_g can also be used to examine the impact of filler loading and silane surface treatments. As shown in Figure 5, T_g of BECy decreases by up to 13.5 and 14.5 °C upon the incorporation of 10 and 20

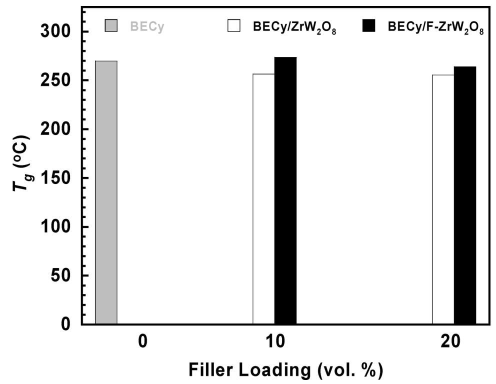

FIGURE 5. Effect of ZrW_2O_8 and F-ZrW_2O_8 loading on T_g.

vol % ZrW_2O_8 particles, respectively; however, the T_g reduction is substantially mitigated upon performing silane treatment of ZrW_2O_8. Upon the incorporation of 10 vol % F-ZrW_2O_8, the T_g of the composite increases by 3.9 °C compared to BECy. Upon the incorporation of 20 vol % F-ZrW_2O_8, T_g is found to be reduced by 6 °C compared to BECy, which is a significant improvement compared to untreated particles at the same loading. The enhancement in T_g could be due to the improved compatibility of F-ZrW_2O_8 with the BECy polymer matrix as a consequence of silane surface treatment.

The dynamic DSC curing measurements for the neat BECy resin and BECy/ZrW_2O_8 composites are shown in Figure 6a–d. The value of ΔH for BECy is found to be 699.1 J/g (92.2 kJ/cyanate equivalent), which is consistent with the values obtained in our previous work (2) with BECy and also in the range reported in the literature for other cyanate ester resins (30, 31). ΔH does not vary systematically with the filler loading and has an average value of 691.2 J/g (91.2 kJ/cyanate equivalent) for the ZrW_2O_8-reinforced resins The cure onset and peak temperatures obtained from the exotherms in Figure 6 are plotted as a function of the heating rate in Figures 7 and 8, respectively. The exotherm onset and peak temperatures for BECy/ZrW_2O_8 composites are found to be significantly lower than the corresponding values for the neat BECy resin at every heating rate. Furthermore, the values of the onset and peak temperatures exhibit a systematic decrease with increasing ZrW_2O_8 loading. The decrease in both the onset and peak temperatures with ZrW_2O_8 loading is indicative of a significant increase in the cure rate. It is noted that the values of the onset and peak temperatures for BECy/F-ZrW_2O_8 are also lower than the corresponding values for BECy, indicating an increase in the cure rate upon the incorporation of F-ZrW_2O_8. Furthermore, the onset temperatures for the composite with 20 vol % F-ZrW_2O_8 are found to be higher than the values for the composite with 20 vol % as-received ZrW_2O_8 at any heating rate. Hence, the experiments demonstrate that, at the same loading, silane treatment of ZrW_2O_8 results in a delay in the onset of BECy cure in comparison with untreated ZrW_2O_8. Although the peak temperatures for the composite with F-ZrW_2O_8 are found to be higher than the values for the composite with untreated ZrW_2O_8 at the slower heating rates of 7 and 5 K/min, no difference can be observed in the values at higher heating rates.

The increase in the cure rate of BECy observed upon the incorporation of ZrW_2O_8 is believed to be due to the presence and nature of hydroxyl groups on the filler particle surface. The presence of hydroxyl groups is confirmed by the FT-IR measurements of ZrW_2O_8 shown in Figure 9, in which the peak observed around 3500 cm^{-1} corresponds to the stretching of hydroxyl groups. The FT-IR data of F-ZrW_2O_8 shown in Figure 9 are similar to the spectrum of as-received ZrW_2O_8. Although the TGA and DSC measurements demonstrate the effect of silane treatment on the ZrW_2O_8 particles, the differences are not captured in the FT-IR spectra because of the occurrence of a large peak, possibly due to ZrO_2 in the region (700 cm^{-1}) where the peaks of silane groups are expected. The catalytic effect of surface hydroxyl groups on the BECy resin observed in this work is consistent with previous work in our laboratory, in which the addition of silica (4) or alumina (5) that contain surface hydroxyl groups increased the curing rate of BECy. The surface hydroxyl groups can react with BECy and form a covalent bond between the particle and the polymer matrix, leading to the observed increase in the cure rate (4). The silane surface treatment involves a replacement of the OH groups with O–Si bonds and, hence, the concentration of hydroxyl groups is reduced in the F-ZrW_2O_8 particles, leading to a delay in the onset of cure when compared with BECy/ZrW_2O_8 composites.

The effect of the ZrW_2O_8 filler particles on the cure behavior of the composites may be further explored using phenomenological reaction models. The use of phenomenological models may involve shortcomings such as a lack of the physical meaning of model parameters; however, it is widely acknowledged that such models capture the essential features of the resin cure behavior (32). In the model calculations, the rate of cure is expressed as a function of the degree of cure, $f(\alpha)$, and a temperature-dependent rate constant, $K(T)$, as shown in eq 2:

$$\frac{d\alpha}{dt} = f(\alpha)\,K(T) \tag{2}$$

In previous work by Sheng and Kessler (2), a wide range of isothermal and dynamic cure measurements of BECy were found to be well described by the autocatalytic model shown below:

$$f(\alpha) = (1 - \alpha)^n \alpha^m \tag{3}$$

where n and m are fit parameters of the reaction order. Finally, substituting the Arrhenius expression for rate constant $K(T) = A\exp(-E_a/RT)$ and the heating rate $\beta = dT/dt$ gives the rate of cure with respect to the temperature, as shown by eq 4.

$$\frac{d\alpha}{dT} = \frac{A}{\beta}\exp\left(\frac{-E_a}{RT}\right)(1 - \alpha)^n \alpha^m \tag{4}$$

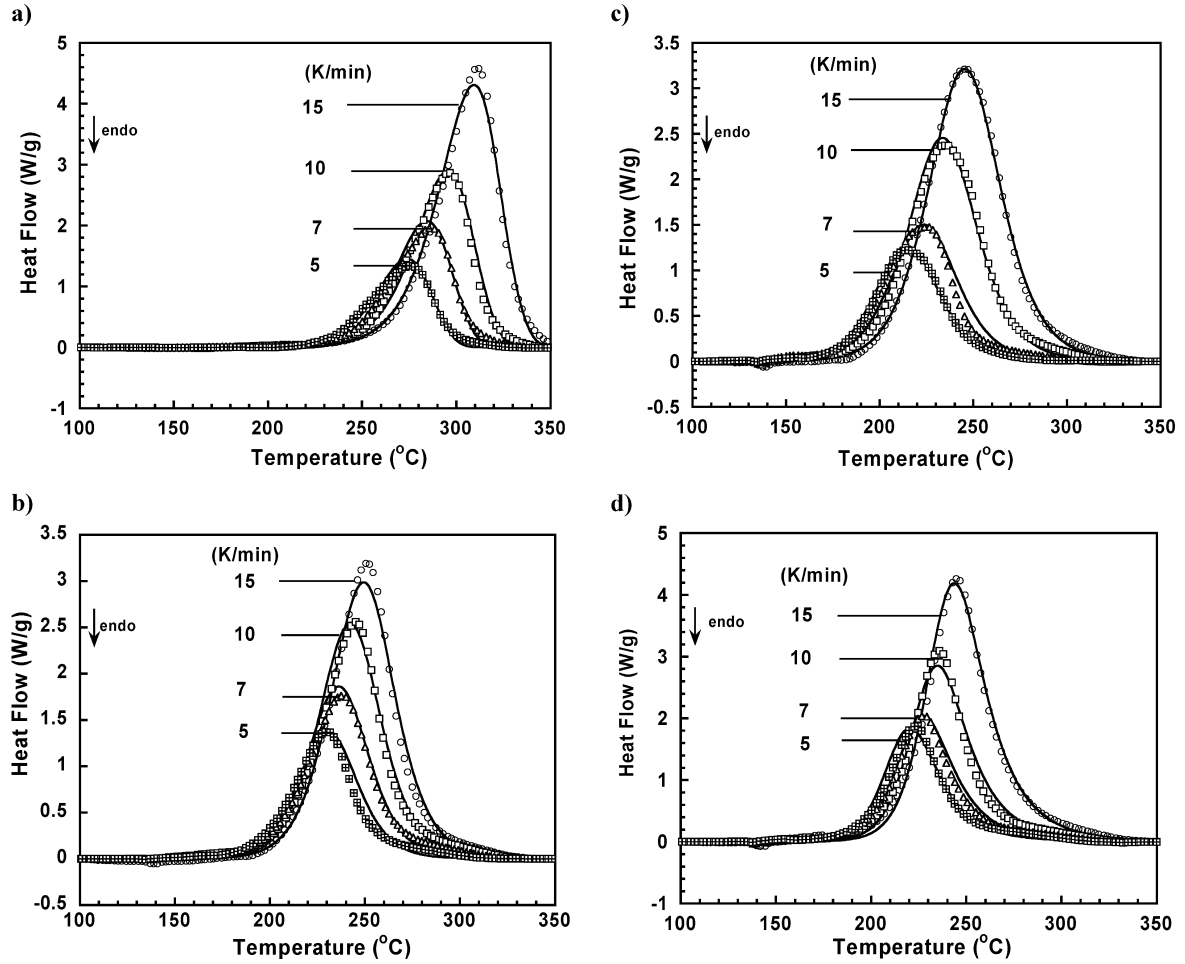

FIGURE 6. Dynamic DSC measurements at various heating rates for (a) BECy, (b) BECy/10 vol % ZrW_2O_8, (c) BECy/20 vol % ZrW_2O_8, (d) BECy/20 vol % F-ZrW_2O_8. The experimental data are represented by symbols, and the solid lines are fits using an autocatalytic reaction model.

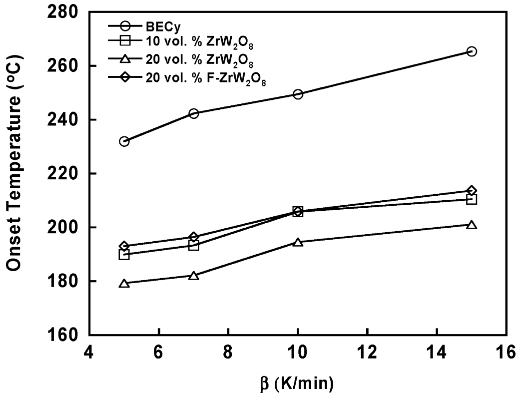

FIGURE 7. Comparison of the onset temperatures (T_o) for the BECy resin and composites as a function of the heating rate.

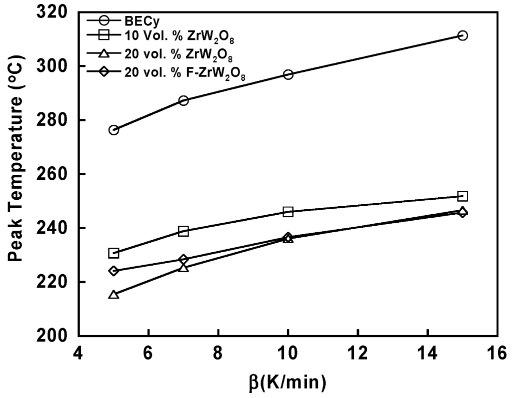

FIGURE 8. Comparison of the peak temperatures (T_p) for the BECy resin and composites as a function of the heating rate.

In eq 4, E_a represents the activation energy of the cure reaction. The fits of the autocatalytic model to the experimental curves are shown as solid lines in Figure 6a–d. The model is found to provide an excellent fit to the experimental data, and the kinetic parameters are tabulated in Table 1. The fact that the same autocatalytic model can describe the cure of BECy, the catalytic effect of the ZrW_2O_8 particles, and the delay in the cure as a consequence of silane surface treatment indicates that the overall reaction mechanism is not significantly altered upon the incorporation of filler particles. The delay in the cure behavior of BECy upon the incorporation of F-ZrW_2O_8 is likely a result of partial steric shielding of the catalyzing hydroxyl groups on ZrW_2O_8 by the silane groups in GPS and is consistent with the higher onset temperatures shown in Figure 7 for these systems. These differences in the cure behavior of BECy as a consequence of the filler loading and type need to be accounted for to optimize the thermomechanical properties of the composites.

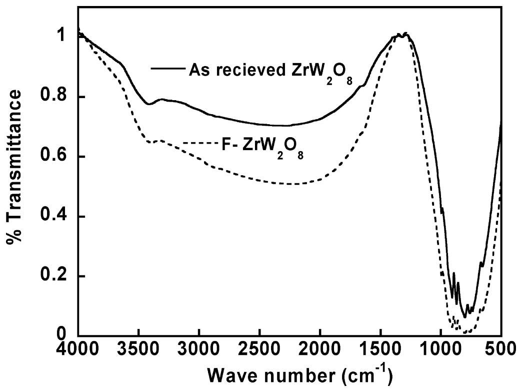

FIGURE 9. FT-IR scans of as-received ZrW_2O_8 and F-ZrW_2O_8 particles.

Table 1. Kinetic Parameters Obtained from an *n*th-Order Autocatalytic Model Fit

sample	log *A* (s^{-1})	E_a (kJ/mol)	*n*	*m*
BECy	4.89	74.2	0.87	0.58
10 vol % ZrW_2O_8	10.27	119.8	1.51	0.32
20 vol % ZrW_2O_8	5.04	67.3	1.36	0.55
20 vol % F-ZrW_2O_8	7.78	92.6	1.8	0.58

4. CONCLUSIONS

In this work, the impact of the zirconium tungstate filler particles on the cure behavior of BECy was examined by dynamic DSC measurements. The cure of BECy is expedited upon the incorporation of ZrW_2O_8, indicative of a catalytic effect of the particles. The catalytic effect is found to increase with increasing loading of the ZrW_2O_8 filler loading. The increase in the cure rate of BECy with the filler loading is believed to be due to the presence and nature of surface hydroxyl groups on the ZrW_2O_8 particles. The reduction in T_g observed upon filler loading in BECy/ZrW_2O_8 composites was substantially mitigated when the ZrW_2O_8 particles were functionalized with silane surface treatment. Although the silane-treated ZrW_2O_8 particles were also found to catalyze the cure of BECy, the dynamic DSC experiments indicate that the onset of the cure is delayed in comparison with that of BECy/ZrW_2O_8 composites of the same loading. The cure behaviors of BECy/ZrW_2O_8 and BECy/F-ZrW_2O_8 composites were found to be well described by an autocatalytic reaction model, which indicates that, in spite of differences in cure kinetics, the overall mechanism of the BECy cure is not significantly altered upon the incorporation of ZrW_2O_8 particles.

Acknowledgment. Financial support from the Air Force Office of Scientific Research (AFSOR), the Department of Energy's Science Undergraduate Laboratory Internship (SULI) program at Ames Laboratory, and a National Science Foundation Research Experience for Undergraduates (NSF REU) is gratefully acknowledged. We thank Cory Sents (Materials Science and Engineering, Iowa State University) for his assistance with DSC measurements. We also thank Dr. Xia Sheng (Materials Science and Engineering, Iowa State University) for his assistance with the GPS functionalization as well as thoughtful discussions.

Supporting Information Available: TGA of composites and XRD spectra of zirconium tungstate powders. This material is available free of charge via the Internet at http://pubs.acs.org.

REFERENCES AND NOTES

(1) Goertzen, W. K.; Kessler, M. R. *Composites, Part A* **2007**, *38*, 779.
(2) Sheng, X.; Akinc, M.; Kessler, M. R. *J. Therm. Anal. Calorim.* **2008**, *92*, 77.
(3) Shimp, D. A.; Craig, W. M., Jr. *Proc. 34th Annu. Int. SAMPE Symp.* **1989**, 1336.
(4) Goertzen, W. K.; Sheng, X.; Akinc, M.; Kessler, M. R. *Polym. Eng. Sci.* **2008**, *48*, 875.
(5) Sheng, X. Ph.D. Thesis, Iowa State University, Ames, IA, 2008.
(6) Goertzen, W. K.; Kessler, M. R. *J. Therm. Anal. Calorim.* **2008**, *93*, 87.
(7) Bansal, A.; Yang, H.; Li, C.; Benicewicz, B. C.; Kumar, S. K.; Schadler, L. S. *J. Polym. Sci., Polym. Phys.* **2006**, *44*, 2944.
(8) Ganguli, S.; Dean, D.; Jordan, K.; Price, G.; Vaia, R. *Polymer* **2003**, *44*, 6901.
(9) Kissounko, D. A.; Deitzel, J. M.; Doherty, S. P.; Shah, A.; Gillespie, J. W. *Eur. Polym. J.* **2008**, *44*, 2807.
(10) Patel, H.; Parikh, A.; Chudasama, U. *Bull. Mater. Sci.* **2005**, *28*, 137.
(11) Sleight, A. W. *Annu. Rev. Mater. Sci.* **1998**, *28*, 29.
(12) Evans, J. S. O.; Jorgensen, J. D.; Short, S.; David, W. I.; Ibberson, R. M.; Sleight, A. W. *Phys. Rev. B* **1999**, *60*, 14643.
(13) Drymiotis, F. R.; Ledbetter, H.; Betts, J. B.; Kimura, T.; Lashley, J. C.; Migliori, A.; Ramirez, A. P.; Kowach, G. R.; Van Duijn, J. *Phys. Rev. Lett.* **2004**, *93*, 025502.
(14) Jorgensen, J. D.; Hu, Z.; Teslic, S.; Argyriou, D. N.; Short, S.; Evans, J. S. O.; Sleight, A. W. *Phys. Rev. B* **1999**, *59*, 215.
(15) Shi, J. D.; Pu, Z. J.; Wu, K.-H.; Larkins, G. *Proc. Mater. Res. Soc. Symp.* **1997**, 229.
(16) Weyer, W. C.; Cross, W. M.; Henderson, B.; Kellar, J. J.; Kjerengtroen, L.; Welsh, J.; Starkovich, J. *Proc. 46th AIAA/ASME/ASCE/AHS/ASC Conf.* **2005**, 3577.
(17) Miller, W.; Smith, C. W.; Dooling, P.; Burgess, A. N.; Evans, K. E. *Phys. Status Solidi B* **2008**, *245*, 552.
(18) Sullivan, L. M.; Lukehart, C. M. *Chem. Mater.* **2005**, *17*, 2136.
(19) Tani, J. I.; Kimura, H.; Hirota, K.; Kido, H. *J. Appl. Polym. Sci.* **2007**, *106*, 3343.
(20) Kessler, M. R.; White, S. R. *J. Polym. Sci., Polym. Chem.* **2002**, *40*, 2373.
(21) Chen, C. C.; Dom, T. N.; Lin, T. H.; Cheng, L. P. *J. Appl. Polym. Sci.* **2004**, *92*, 3067.
(22) Nair, C. P. R.; Mathew, D.; Ninan, K. *Adv. Polym. Sci* **2001**, *155*, 1.
(23) De Meyer, C.; Vandeperre, L.; Van Driessche, I.; Bruneel, E.; Hoste, S. *Cryst. Eng.* **2002**, *5*, 469.
(24) Holzer, H.; Dunand, D. C. *J. Mater. Res.* **1999**, *14*, 780.
(25) Evans, J. S. O.; Hu, Z.; Jorgensen, J. D.; Argyriou, D. N.; Short, S.; Sleight, A. W. *Science* **1997**, *275*, 61.
(26) Cross, W. M.; Henderson, B. D.; Weyer, W. C.; Kroetch, C.; Kjerentroen, L.; Welsh, J.; Kellar J. J. Functional fillers for dimensional stability. In *Functional Fillers and Nanoscale Minerals*; Kellar, J. J., Ed.; Society for Mining, Metallurgy & Exploration: Littleton, CO, 2006; pp 127−140.
(27) Sleight, A. W.; Evans, J. S. O.; David, W. I. F. *Acta Crystallogr.* **1999**, *B55*, 333.
(28) Perottoni, C. A.; Da Jornada, J. A. H. *Science* **1998**, *280*, 886.
(29) Abboud, M.; Turner, M.; Duguet, E.; Fontanille, M. *J. Mater. Chem.* **1997**, *7*, 1527.
(30) Harismendy, I.; Gomez, C. M.; Del Rio, M.; Mondragon, I. *Polym. Int.* **2000**, *49*, 735.
(31) Gomez, C. M.; Recalde, I. B.; Mondragon, I. *Eur. Polym. J.* **2005**, *41*, 2734.
(32) Hale, A. In *Handbook of Thermal Analysis and Calorimetry*; Cheng, S. Z. D., Ed.; Elsevier: New York, 2002; Vol. 3, Chapter 9, pp 295−353.

AM900051G